



Microstructure and bending piezoelectric characteristics of AlN film for high-frequency flexible SAW devices

Kaixuan Li¹, Fang Wang^{1,2}, Meng Deng¹, Kai Hu¹, Dianyou Song^{1,*}, Yaowu Hao², Huanhuan Di¹, Kaifei Dong¹, Shuo Yan¹, Zhitang Song³, and Kailiang Zhang^{1,*}

¹Tianjin Key Laboratory of Film Electronic & Communication Devices, School of Electrical & Electronic Engineering, Tianjin University of Technology, Tianjin 300384, China

²Department of Materials Science and Engineering, University of Texas At Arlington, Arlington, TX 76019, USA

³State Key Laboratory of Functional Materials for Informatics, Shanghai Institute of Micro-System and Information Technology, Chinese Academy of Sciences, Shanghai 200050, P. R. China

Received: 4 December 2020

Accepted: 23 March 2021

Published online:

7 May 2021

© The Author(s), under exclusive licence to Springer Science+Business Media, LLC, part of Springer Nature 2021

ABSTRACT

Flexible surface acoustic wave (SAW) device is one of hot point areas for wearable communication technology because of their ductility and bendability, but the deterioration problem of device performance after bending experiments is limiting its wide application for future wearable communication devices. In this work, the effect of sputtering power on microstructure properties and bending piezoelectric characteristics of aluminum nitride (AlN) film on polyimide (PI) with molybdenum (Mo) buffer layer for high-frequency flexible SAW device was discussed in detail from 200 W to 280 W. Microstructure results show that the high oriented (002) AlN films with narrow full width at half maximum (FWHM) of 0.29° and low roughness of 3.2 nm are obtained under 240 W sputtering power. Piezoelectric and frequency results of SAW devices after cyclic bending indicate that the relative piezoelectric coefficient d_{33}^* is about 8.01 pm/V, and the center frequency of the flexible SAW devices is as high as 4.95 GHz, especially the piezoelectric and frequency characteristics can maintain high satiability after 10,000 bending cycles. This work may be of useful for the flexible high-frequency SAW devices in the wearable communication area.

Address correspondence to E-mail: youdiansong@163.com; kailiang_zhang@163.com

1 Introduction

Potential application of flexible and wearable functional electronics with good compatibility and stability in human body has attracted widespread attention [1, 2]. The rapid development of real-time communication wearable equipment puts forward higher requirements for bendable, high frequency, and sensitivity communication devices. Piezoelectric materials introduced into flexible device architectures can further expand flexible electronic devices applications to both energy harvesting and bending resistance [3, 4]. Aluminum nitride (AlN) is a piezoelectric ceramic material with good piezoelectric properties. C-axis-oriented AlN thin film prepared on polyethylene terephthalate at room temperature has been used to fabricate stress sensor which frequencies respond from 0.3 Hz to over 100 Hz [5]. FBARs consisting of Mo/AlN/Mo-layered structures were fabricated on a polyimide (PI) substrate [6]. The flexible SAW devices made by combining AlN piezoelectric film with flexible substrate own bendability, good thermal conductivity, and ductility [7]. However, current challenges are the growth of high-quality piezoelectric film on a polymeric flexible substrate and serious deterioration of device performance caused by excessive bending times [8, 9].

It is noteworthy to mention that PI flexible substrate has the prospect of being able to low cost and good mechanical properties (bending strength at room temperature ≥ 170 MPa, tensile strength ≥ 100 MPa). Therefore, AlN film deposited on PI substrate with smaller surface roughness for flexible SAW devices will add flexibility to the design of technology for practical application, due to the simple device structure and low cost [10, 11]. AlN film grown directly on PI substrate has poor crystallinity, but it can be improved by annealing or adding underlying metal as buffer layer, or by controlling the Al content to improve the confinement of the two-dimensional electron gas to optimize a good interface [12], which has a significant effect on the c-axis orientation and piezoelectric properties of AlN film [13]. Depositing the AlN/metal stack onto a polymer substrates should enhance the piezoelectric coefficients of the AlN film [14]. The lattice mismatch coefficient between Mo (110) and AlN film is only 0.87% [15], so Mo film is selected as a buffer layer to promote AlN film growth oriented along the c-axis perpendicular to flexible substrate [16–18]. Reactive magnetron

sputtering can produce high-quality AlN films with guaranteed uniformity of film thickness and low surface roughness [19–21].

In this work, the AlN film on PI substrate has excellent c-axis orientation and maintenance of bending properties by inserting the Mo-buffered layer and optimizing the power of the magnetron sputtering. Especially, the piezoelectric and frequency characteristics can maintain high satiability after 10,000 bending cycles, and the d_{33}^* value reported in this work has the largest value for a flexible AlN film on PI of 8.01 pm/V compared to the high of around 4.87 pm/V reported by Nathan Jackson et al. [13], which are attributed to the preferential orientation along c-axis and good crystal quality of the obtained AlN films. These results imply that the potential of using the AlN/Mo/PI composite structures in flexible SAW applications.

2 Experimental

AlN thin films were deposited on 50- μm -thick PI substrates through inserting the 200-nm-thick Mo film buffer layer using a DC reactive magnetron sputtering system at room temperature. The targets were 60 mm diameter, 99.999% pure Mo, and Al disks, respectively, and distance between the substrate and target was about 45 mm. Before depositing AlN film, (110) oriented Mo thin film was deposited on PI substrate as a buffer layer, with sputtering pressure of 1.0 Pa, sputtering power of 100 W, and argon flow of 40 sccm. AlN films with (002) preferred orientation were optimized after studying growth mechanism. The total gas flux rate during deposition process was maintained at a constant of 40 sccm, where the flux ratio of Ar (99.999% pure) and N_2 (99.999% pure) gases was 1:2, and deposition pressure was maintained at 0.3 Pa at ambient temperature. The sputtering power is changed from 200 W to 280 W to optimize the growth process of the AlN film and maintain its thickness constant at 800 nm.

Thicknesses of Mo and AlN films were estimated using a Dektak Veeco 150 profilometer. Crystal orientation of the films was investigated by X-ray diffraction (XRD, Rigaku-Ultima IV) using $\text{Cu-K}\alpha$ radiation. The Al and N concentrations were analyzed by X-ray energy dispersive spectrometers (EDS, Oxford Instruments). The surface morphology characterizations of AlN films were examined by atomic

force microscopy (AFM, Agilent 5500) in contact mode. The piezoelectric properties were, respectively, analyzed by piezoresponse force microscopy (PFM, Agilent 5500) and cyclic bending tester.

To evaluate the piezoelectric and acoustic properties of deposited AlN films, SAW devices were realized in a resonator configuration. The IDTs consisted of an 80-nm-thick titanium (Ti) film were structured by electron-beam lithography (EBL, Raith) and electron-beam evaporation (SKY EB500-I), polymethyl methacrylate (PMMA) was used as a mask in this process. The SAW devices were finally obtained by lift-off technique. Frequency responses of the IDT/AlN/Mo/PI composite structure were tested by a network analyzer (Keysight PNA N5232A) and a radio frequency (RF) microprobe equipped with ground-signal-ground (G-S-G) probe.

3 Results and discussion

Figure 1 shows the obtained crystallinity results. It is clear that all samples have the (002) orientation of AlN films. XRD patterns of the AlN films grown at different sputtering powers on Mo film are shown in the left part of Fig. 1, two obvious diffraction peaks are observed, namely AlN (002) at $2\theta \approx 36.08^\circ$ and Mo (110) at $2\theta \approx 40.74^\circ$. The presence in the spectrum of the (002) peak confirms the preferential orientation of the AlN film. A slight shift of the peak towards higher 2θ angle respect to the bulk $2\theta = 36.03^\circ$ value can be noted, indicating a film growth in-plane compressive strain due to unit cell distortion. The XRD

intensity of AlN (002) peak first increases and then decreases with increasing sputtering power, and reaches the maximum values at a sputtering power of 240 W. The corresponding full width at half maximum (FWHM) of the AlN (002) peak can be observed on the right part of Fig. 1, which reaches a minimum value of 0.29° at 240 W when the sputtering power was varied between 200 W and 280 W. Narrow peaks confirm the c-axis highly oriented texture of piezoelectric layer, and it is very important to enhance the piezoelectric coefficient of the material.

XRD analysis is aimed to verify the preferential orientation of the AlN film along the c-direction. In the hexagonal wurtzite structure of AlN, each Al atom is surrounded by four N atoms to creating a tetrahedral structure. Three short-bonded N atoms (B1 bond) are located on the c-plane while a long-bonded N atom (B2 bond) is located in the vertical direction along the c-axis. The c-axis is the polar axis, and the wurtzite crystal structure is non-centrosymmetric only along the c-direction. Therefore, AlN exhibits the highest piezoelectric response when the growth axis coincides with the (002) crystal direction. Appropriate sputtering growth conditions facilitate the arrangement of target atoms with preferential orientation along c-axis after arriving on the substrate. The effect of deposition power on the properties of AlN films was examined by varying one parameter while holding the remaining ones fixed. In the hexagonal AlN cell, the binding energy of B2 bond along the c-axis is less than that of B1 bond and the surface energy of the (002) face is slightly lower than that of the other faces. Sputtering power is the

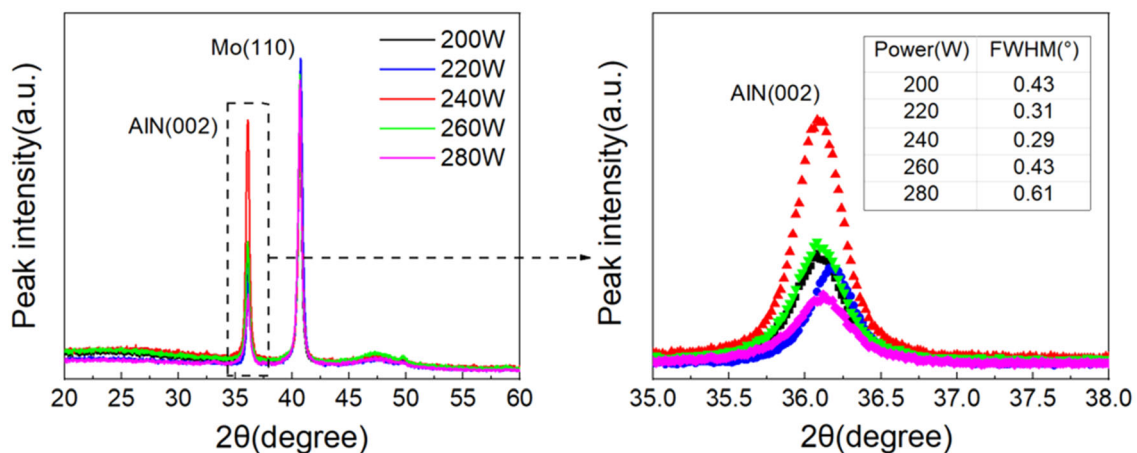


Fig. 1 Effect of different sputtering power on (002) crystal direction and FWHM of AlN (002) peak. Left: XRD spectra, right: amplified AlN (002) peak and FWHM of the AlN (002) peak as a function of sputtering power

main energy source of sputtered atoms. Appropriately increasing sputtering power can improve crystal quality and promote (002) preferred orientation growth. When the sputtering power values are lower than 240 W, as the sputtering power increases, the aluminum (Al) atoms reaching the substrate have higher kinetic energy, which enables the Al atoms to be sufficiently relaxed near the deposition location and move to a position where the system energy can be reduced. As a result, the (002) oriented grains with lower surface energy are more likely to grow. Therefore, higher sputtering power contributes to the enhancement of AlN (002) peak intensity. But when the sputtering power is greater than 240 W, the high-energy incident atoms destroy the newly formed AlN layer and reduce the adatom diffusion length, thus, deteriorating the (002) orientation. The FWHM is also an important parameter to evaluate AlN piezoelectric films quality. The smaller the FWHM, the more preferred the c-axis orientation of AlN films, indicating that the alignment of the crystal grains perpendicular to the substrate is better. We can conclude that the c-axis preferential orientation is improved significantly by optimizing sputtering power, and optimal structure is achieved with the sample AlN-240 W.

Figure 2 shows the influence of different sputtering powers on the content of elements in the AlN films analyzed by EDS. Figure 2a displays that with the increase of sputtering power, N at% / Al at% (N at% is the atomic percentage of N atom, Al at% is the atomic percentage of Al atom) decreases gradually. The sputtering power affects the activation energy of the sputtering Al atoms and the N atoms formed by the ionization of nitrogen. When the sputtering power is as low as 200 W, the sputtered Al atoms and the N atoms formed by ionization are both less, and the activation energy is low. The sputtered Al atoms need to pass the distance between the target and substrate to reach the surface of the films, while N atoms are relatively close to the films surface. There are more N atoms adsorbed to the surface of Mo films than Al atoms, so N-rich AlN films are formed. When the sputtering power is as high as 280 W, a large number of Al atoms on the surface of the target are sputtered out. Since the activation energy transferred by the collision of Ar ions to Al atoms is greater than that of N atoms, there are more Al atoms than N atoms adsorbed on the surface of Mo film. Redundant Al atoms adsorbed on the surface of AlN films do not react with the unsaturated bonds and gather

on the films surface, thus, forming the Al-rich AlN films. For ideal sputtering, if all the sputtered Al elements are combined with the N elements to form AlN, the N at% / Al at% would just be 1:1 in the films. Figure 2a shows that the N at% / Al at% is close to 1:1 at the sputtering power of 240 W, and the EDS surface scan map at this condition is shown in Fig. 2b. And Fig. 2c–e illustrates that both the N elements and the Al elements are uniformly distributed in the surface scan map, indicating that the element composition in the AlN films is uniform. It also contains oxygen elements in the AlN films as shown in Fig. 2d, which is due to the residual oxygen in the chamber or the films being oxidized during storage to form the Al₂O₃ films.

It is important to examine the morphology of AlN films deposited on the Mo films which previously prepared on PI substrates for the preparation process and performance stability of the device in the next step. From Fig. 3, with the increase of sputtering power (200 ~ 280 W), crystallinity of the prepared AlN thin films is improved, grain grows and becomes larger, and the grain size is uniform and dense. Figure 3a shows the AFM surface scan of AlN films deposited at 200 W. The low power results in the lower energy of Ar ions and N atoms formed by the ionization of argon and nitrogen, and the activation energy of Al atoms generated by the collision of Ar ions with Al target is also relatively small. So the activation energy of Al atoms and N atoms adsorbed on the surface of Mo film is low, which is not conducive to the reaction with unsaturated Al–N bond and the formed AlN film has poor crystallization quality. Figure 3b–e demonstrates that as the sputtering power increases, the atomic energy of N atoms and Al atoms are increased, which lead to the enhanced migration ability of Al atoms and N atoms adsorbed on the surface of Mo film. The Al–N bonds formed by Al atoms, N atoms, and unsaturated bonds increase, which is conducive to the formation of a uniform AlN film surface. It is clear in Fig. 3c that the AlN films have dense grains and excellent surface morphology when the sputtering power is 240 W. When the sputtering power continues to increase to 280 W, the AlN films are excessively crystallized, resulting in abnormal growth of crystal grains and uneven grain size. The grain size is mainly affected by sputtering power and increases with the improvement of power, so the root-mean-square surface roughness (RMS) of the AlN film also

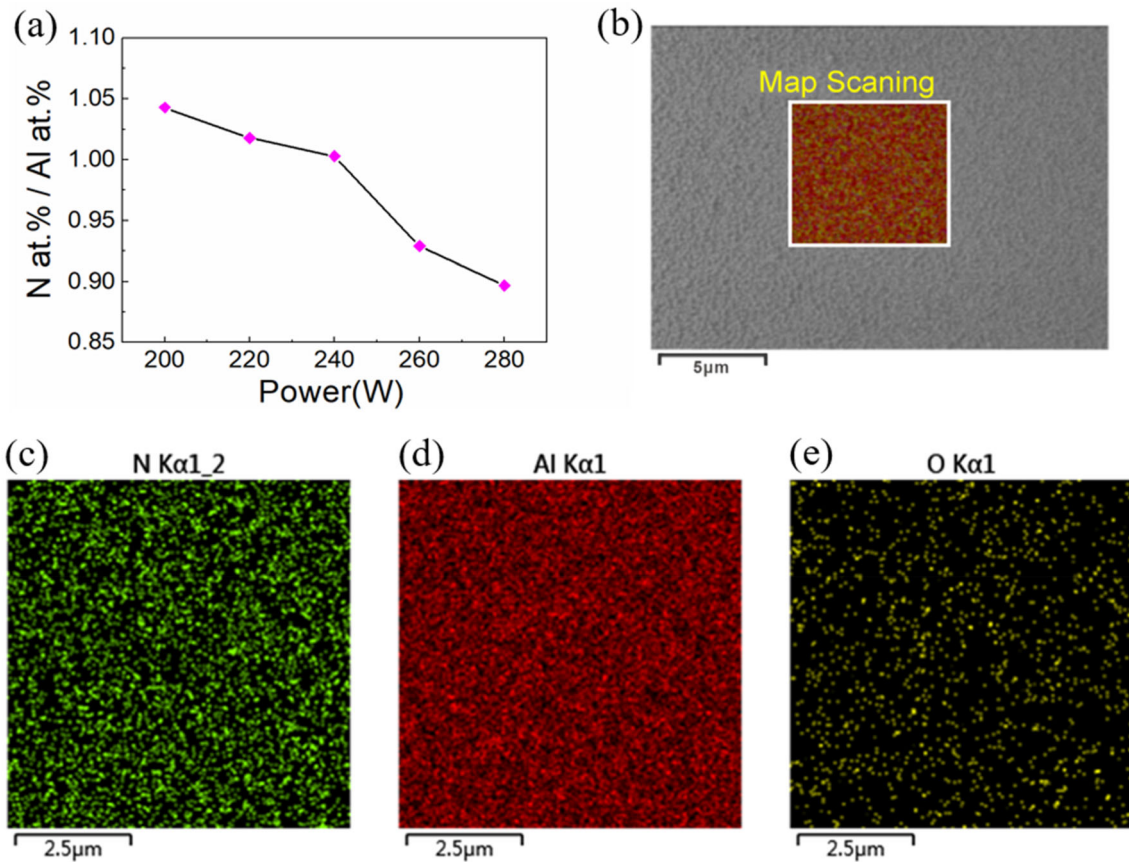


Fig. 2 EDS spectrum of AlN films with 200 W, 220 W, 240 W, 260 W, and 280 W sputtering power. **a** the ratio of the atomic percentage of N element to the atomic percentage of Al element,

b EDS surface scan map when sputtering power is 240 W, **c** distribution map of N element, **d** distribution map of O element, **e** distribution map of Al element

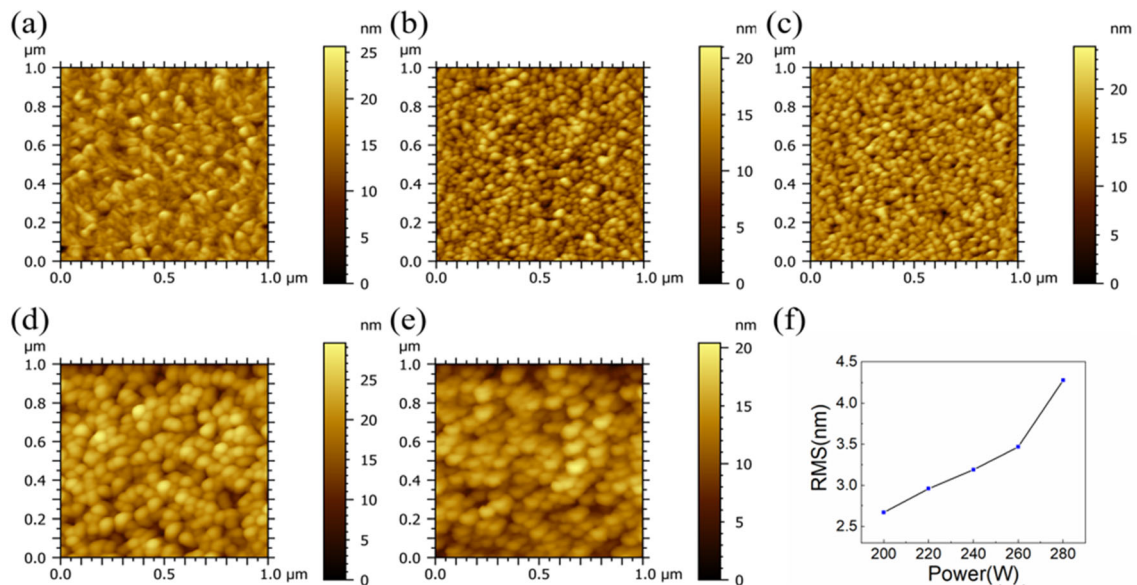


Fig. 3 AFM of AlN films with different sputtering powers. **a** 200 W, **b** 220 W, **c** 240 W, **d** 260 W, **e** 280 W, **f** effect of sputtering power on root-mean-square surface roughness of AlN thin films

gradually increases, as shown in Fig. 3f. Since the surface acoustic wave is only propagated near the surface, all the energy is concentrated nearly within a wavelength distance from the surface. If the surface roughness is higher than the wavelength, the surface acoustic wave will not be able to propagate properly. It is reported that the surface roughness of the piezoelectric films has to be less than 30 nm for GHz-grade SAW devices. The RMS of AlN film is about 3.2 nm at the sputtering power of 240 W, which meets the requirement of SAW device preparation.

Figure 4 depicts the micro-area piezoelectric properties of the AlN films deposited on Mo/PI flexible substrate at 240 W in different bending times. The PFM module of Agilent 5500 AFM system was used to characterize the piezoelectric properties of AlN thin films. Due to the inverse piezoelectric effect, a deformation in AlN films appeared under the action of electric field between the conductive probe and the bottom electrode of the sample, the variation between deformation amplitude and pre-set voltages is recorded as a butterfly curve. The piezoelectric properties of AlN films are represented by butterfly curve and relative piezoelectric coefficient (d^*_{33}).

d^*_{33} curve is calculated by formula (1):

$$d^*_{33} = (A_i - A_0)/(V_i - V_0), \tag{1}$$

where, (A_i, V_i) is the amplitude and voltage at any single point in the butterfly curve and (A_0, V_0) is the intersection of the butterfly curve [22]. Figure 4a–c shows butterfly curves of AlN films at different bending times and relative piezoelectric coefficient (d^*_{33}) curves calculated using Eq. (1). By applying an alternating voltage of -10 V to $+10\text{ V}$ to -10 V between the conductive probe and the bottom electrode of sample, the generated electric field causes the piezoelectric material to deform. The external alternating electric field polarizes the internal charge of piezoelectric film, and electric field strength increases gradually from 0, so that polarization intensity increases to a certain value. At this time, the electric field is gradually reduced, and the partial arrangement of charge is still maintained, so change of polarization strength always lags behind the change of electric field strength, in other words, the change of amplitude strength lags behind the change of electric field strength. According to Fig. 4a, in the unbent condition, it can be seen that the relative

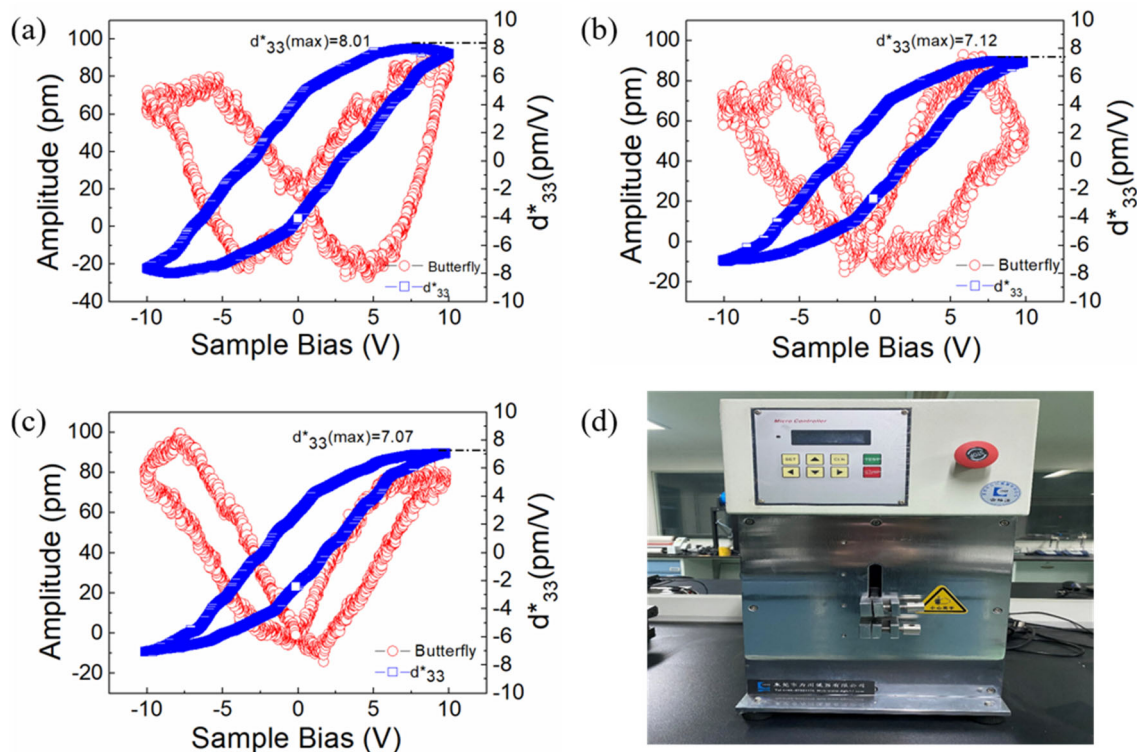


Fig. 4 PFM spectrum of AlN films prepared at 240 W. Butterfly curve measured and the corresponding piezoelectric coefficient spectrum: **a** AlN film was not bent, **b** bending 5000 times, **c** bending 10,000 times, **d** the bending tester used for cyclic bending test

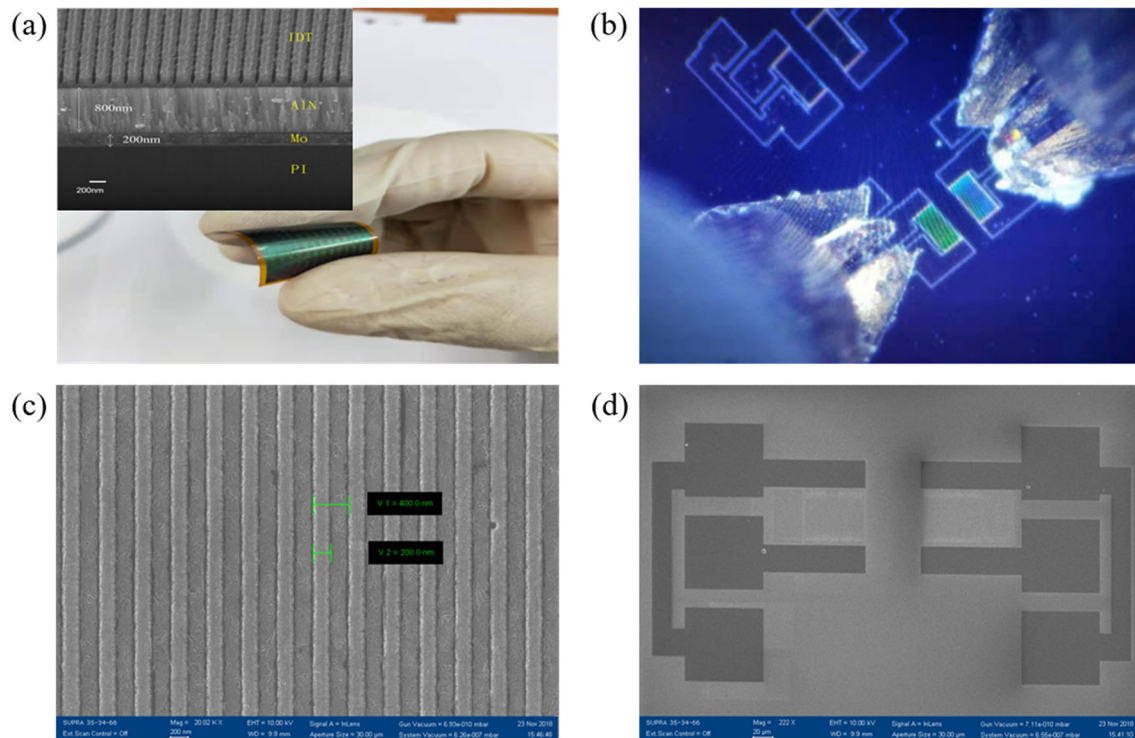


Fig. 5 Device fabrication. **a** IDTs devices fabricated on AlN thin films, inset: SEM cross-sectional image of the IDT/AlN/Mo /PI-stacked layer, **b** IDTs device test frequencies for prepared G-S-G structures, **c** and **d** SEM images of 200 nm IDTs devices

piezoelectric coefficient d_{33}^* (pm/V) of AlN film has a relatively full curve window with the change of bias voltage and d_{33}^* (max) = 8.01 pm/V, indicating that the AlN film deposited at 240 W after power optimization has a good piezoelectric response characteristic and a strong piezoelectric effect. Relative piezoelectric coefficient d_{33}^* is a characterization of the relationship between stress and generated charge of piezoelectric materials. The higher piezoelectric constant of the general film, the better piezoelectric performance.

Figure 4d is the photo of the bending tester with a curvature of 45° , a bending radius of 25.47 mm, and the arc length $L = \alpha$ (radian) $\times r$ (radius) that was calculated to be 20 mm. The stability of the piezoelectric properties of the prepared AlN/Mo/PI composite structure was explored after cyclic bending. The selected PI substrate has excellent mechanical properties, and both ductility and flexibility can withstand the experimental requirements. The cyclic bending times were 0, 5000, and 10,000 times, respectively. Clearly shown in Fig. 4b–c, the window of butterfly curve decreases with the increase of cyclic bending times, and the maximum values of relative piezoelectric coefficient d_{33}^* (pm/V) are 7.12 and 7.07

at 5000 and 10,000 times, respectively, which decrease slightly and remain stable. Because of tens of thousands of cyclic bending times, the internal lattice cells of AlN film were deformed under the action of stress, and the arrangement along the c-axis direction was shifted to some extent, which leading to the decline of piezoelectric performance. When the voltage was applied to the surface of the AlN film, the polarization intensity of the internal charge of the piezoelectric film was weakened and the amplitude dropped. So the piezoelectric coefficient d_{33}^* also decreased, but the change was not significant. The test results indicate that the AlN film deposited at 240 W through inserting Mo film buffer layer has good piezoelectric response characteristic and maintains high stability after 10,000 cycles of bending.

Flexible SAW device with IDT (80 nm)/AlN (800 nm)/Mo (200 nm)/PI (50 μ m) stacked layer structure was constructed as shown in Fig. 5a and the inset is its SEM cross-sectional image. Figure 5b shows that the pad was in contact with corresponding G-S-G microwave probe at the time of measurement, the lower left probe is the SAW generation port, and the upper right probe is the SAW receiving port. The device was consisted of two identical interdigitated

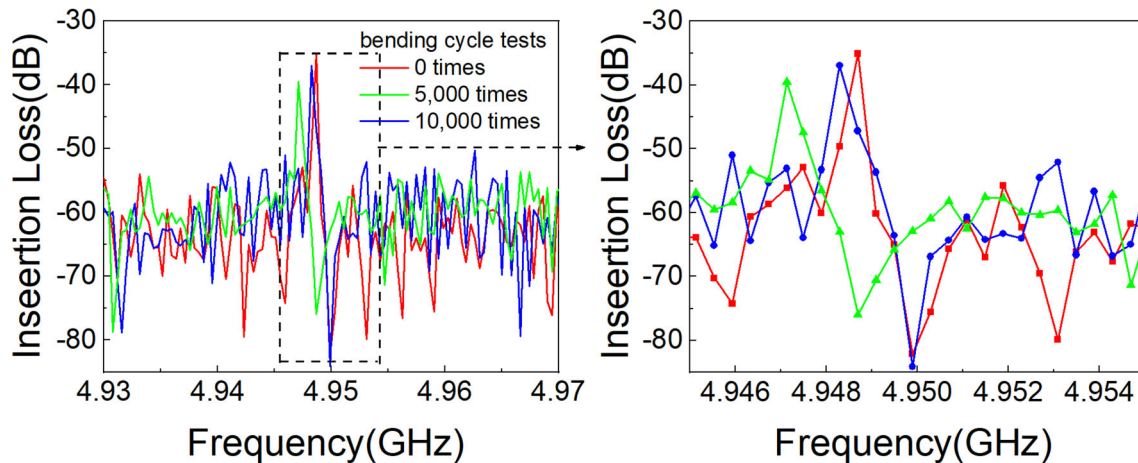


Fig. 6 Frequency response of the SAW device with different bending times. The red curve is the frequency measured before bending, the blue curve is the frequency measured after bending 5000 times, and the green curve is the frequency measured after bending 10,000 times

transducers (IDT) with a wavelength of $\lambda = 800$ nm, $N_p = 50$ (IDT finger pairs), $W = 100\lambda$ (acoustic aperture), and $M = 80\lambda$ (delay distance). The reflectors were used to enhance the strength of standing wave. Obviously shown in Fig. 5c–d that the electrode lines of interdigital electrodes are well prepared which width is the same as the width of the gaps, indicating that the prepared IDTs have a good quality.

Frequency response of the unencapsulated SAW device was tested using multi-function probe station and vector network analyzer, and the results are shown in Fig. 6. The prepared AlN film has a c-axis oriented and a smaller surface roughness to obtain a higher frequency. From Fig. 6, frequency of the 200 nm SAW device is 4.95 GHz and insertion loss is -35.04 dB; the high insertion loss may be caused by parasitic parameters such as actual process parameters and packaging. After cyclic bending for 5000 and 10,000 times, the center frequency decreases slightly but still remains within a range of 4.95 GHz, and the insertion loss drops slightly from -35.04 dB to -39.54 dB due to the minor damage to device during cyclic bending. In general, the frequency response characteristics of device remain stable under high bending times, indicating that the flexible SAW device has good quality and bending performance.

4 Conclusions

In this work, the effect of sputtering power on c-axis oriented, element composition, and surface morphology of AlN films on PI with Mo buffer layer was

investigated in detail from 200 W to 280 W. Both XRD, EDS, and AFM results show that the high oriented (002) AlN films with narrow FWHM of 0.29° , uniform Al and N element distribution (N at% / Al at% = 1), and low roughness of 3.2 nm are obtained under 240 W sputtering power. PFM results indicate that the peak relative piezoelectric coefficient (d_{33}^*) is about 8.01 pm/V and butterfly curve window is relatively full, which confirmed that AlN films on PI with Mo buffer layer deposited at 240 W have uniform piezoelectric performance. The center frequency of the flexible SAW devices with IDTs/AlN/Mo/PI composite structure is as high as 4.95 GHz. Cyclic bending test results especially show that both the piezoelectric and frequency characteristics can maintain high stability after 10,000 bending cycles. This work may have certain reference value for the flexible high-frequency SAW devices in the field of wearable communication.

Acknowledgements

This work was supported by the Natural Science Foundation of Tianjin City (Grant Nos. 18JCZDJC30500, 17JCYBJ C16 100, and 17JCZDJC31700), National Key Research and Development Program of China (Grant No. 2017YFB0405600), and National Natural Science Foundation of China (Grant Nos. 61404091, 61274113, 61505144, 51502203, and 51502204). Science and Technology Planning Project of Tianjin City (20ZYQCGX00070), and Open project of state Key

Laboratory of Functional Materials for Information (SKL202007).

References

1. S. Park, S.W. Heo, W. Lee, D. Inoue, Z. Jiang, K. Yu, H. Jinno, D. Hashizume, M. Sekino, T. Yokota, K. Fukuda, K. Tajima, T. Someya, Self-powered ultra-flexible electronics via nano-grating-patterned organic photovoltaics. *Nature* **561**(7724), 516 (2018). <https://doi.org/10.1038/s41586-018-0536-x>
2. M.A. Signore, G. Rescio, C. De Pascali, V. Iacovacci, P. Dario, A. Leone, F. Quaranta, A. Taurino, P. Siciliano, L. Francioso, Fabrication and characterization of AlN-based flexible piezoelectric pressure sensor integrated into an implantable artificial pancreas. *Sci. Rep.* **9**(1), 17130 (2019). <https://doi.org/10.1038/s41598-019-53713-1>
3. L. Lamanna, F. Rizzi, F. Guido, L. Algieri, S. Marras, V.M. Mastronardi, A. Quattieri, M. De Vittorio, Flexible and transparent aluminum-nitride-based surface acoustic-wave device on polymeric polyethylene naphthalate. *Adv. Electron. Mater.* **5**(6), 1900095 (2019). <https://doi.org/10.1002/aelm.201900095>
4. Q. Li, J. Liu, B. Yang, L.J. Lu, Z.R. Yi, Y.W. Tian, J.Q. Liu, Highly sensitive surface acoustic wave flexible strain sensor. *IEEE Electron Device Lett.* **40**(6), 961–964 (2019). <https://doi.org/10.1109/LED.2019.2909320>
5. M. Akiyama, Y. Morofuji, T. Kamohara, K. Nishikubo, M. Tsubai, O. Fukuda, N. Ueno, Flexible piezoelectric pressure sensors using oriented aluminum nitride thin films prepared on polyethylene terephthalate films. *J. Apply. Phys.* **100**(11), 114318 (2006). <https://doi.org/10.1063/1.2401312>
6. F. Martin, P. Muralt, M.A. Dubois, Process optimization for the sputter deposition of molybdenum thin films as electrode for AlN thin films. *J. Vac. Sci. Technol. A* **24**(4), 946–952 (2006). <https://doi.org/10.1116/1.2201042>
7. B. Peng, D.D. Gong, W.L. Zhang, J.Y. Jiang, L. Shu, Y.H. Zhang, Effects of sputtering parameters on aln film growth on flexible hastelloy tapes by two-step deposition technique. *Materials* **9**(8), 686 (2016). <https://doi.org/10.3390/ma9080686>
8. B. Peng, J.Y. Jiang, G. Chen, L. Shu, J. Feng, W.L. Zhang, X.Z. Liu, Preparation of highly c-axis oriented AlN thin films on Hastelloy tapes with Y2O3 buffer layer for flexible SAW sensor applications. *Funct. Mater. Lett.* **9**(2), 1650023 (2016). <https://doi.org/10.1142/S1793604716500235>
9. C.C. Shan, M. Zhao, D.Y. Jiang, J.M. Sun, Y.H. Duan, Q. Li, M. Li, X. Zhou, N. Wang, X.M. Fei, X.J. Zhao, Improved responsivity of highly reproducible performance ZnO thin film flexible UV photodetectors by piezo-phototronic effect. *J. Mater. Sci. Mater. Electron* **30**(16), 15198–15205 (2019). <https://doi.org/10.1007/s10854-019-01892-y>
10. S. Petroni, C. La Tegola, G. Caretto, A. Campa, A. Passaseo, M. De Vittorio, R. Cingolani, Aluminum Nitride piezo-MEMS on polyimide flexible substrates. *Microelectron. Eng.* **88**(8), 2372–2375 (2011). <https://doi.org/10.1016/j.mee.2011.02.080>
11. Q. Li, H.Y. Liu, G. Li, F. Zeng, F. Pan, J.T. Luo, L.R. Qian, Growth and characterization of polyimide-supported AlN films for flexible surface acoustic wave devices. *J. Electron. Mater.* **45**(6), 2702–2709 (2016). <https://doi.org/10.1007/s11664-016-4420-x>
12. T. Aggerstam, S. Lourdudoss, H.H. Radamson, M. Sjodin, P. Lorenzini, D.C. Look, T. Aggerstam, S. Lourdudoss, H.H. Radamson, M. Sjodin, P. Lorenzini, D.C. Look, Investigation of the interface properties of MOVPE grown AlGaIn/GaN high electron mobility transistor (HEMT) structures on sapphire. *Thin Solid Films* **515**(2), 705–707 (2006). <https://doi.org/10.1016/j.tsf.2006.04.052>
13. N. Jackson, A. Mathewson, Enhancing the piezoelectric properties of flexible hybrid AlN materials using semicrystalline parylene. *Smart Mater. Struct.* **26**(4), 045005 (2017). <https://doi.org/10.1088/1361-665X/aa5d99>
14. N. Jackson, Influence of silicon crystal orientation on piezoelectric textured aluminium nitride deposited on metal electrodes. *Vacuum* **132**, 47–52 (2016). <https://doi.org/10.1016/j.vacuum.2016.07.019>
15. Y.Q. Fu, J.K. Luo, N.T. Nguyen, A.J. Walton, A.J. Flewitt, X.T. Zu, Y. Li, G. McHale, A. Matthews, E. Iborra, H. Du, W.I. Milne, Advances in piezoelectric thin films for acoustic biosensors, acoustofluidics and lab-on-chip applications. *Prog. Mater. Sci.* **89**, 31–91 (2017). <https://doi.org/10.1016/j.pmatsci.2017.04.006>
16. K. Samara, F. Ayazi, Combined capacitive and piezoelectric transduction for high performance silicon microresonators, *IEEE Int. Conf. Micro Electro Mech. Syst., 24th, Cancun, Mexico*, pp. 169–172 (2011). <https://doi.org/10.1109/MEMSYS.2011.5734388>
17. K.B. Chavan, S.V. Desarada, N.B. Chaurse, Influences of substrate temperature and Ar flow on the properties of RF sputtered Mo thin films. *J. Mater. Sci. Mater. Electron.* **31**(13), 10306–10314 (2020). <https://doi.org/10.1007/s10854-020-03578-2>
18. S. Imran, J. Yuan, G. Yin, Y.G. Ma, S.L. He, Influence of metal electrodes on c-axis orientation of AlN thin films deposited by DC magnetron sputtering. *Surf. Interface Anal.* **49**(9), 885–891 (2017). <https://doi.org/10.1002/sia.6237>
19. J.L. Tang, D.W. Niu, Z.W. Tai, X.W. Hu, Deposition of highly c-axis-oriented ScAlN thin films at different sputtering power.

- J. Mater. Sci. Mater. Electron. **28**(7), 5512–5517 (2017). <https://doi.org/10.1007/s10854-016-6213-7>
20. H. Jin, J. Zhou, S.R. Dong, B. Feng, J.K. Luo, D.M. Wang, W.I. Milne, C.Y. Yang, Deposition of c-axis orientation aluminum nitride films on flexible polymer substrates by reactive direct-current magnetron sputtering. *Thin Solid Films* **520**(15), 4863–4870 (2012). <https://doi.org/10.1016/j.tsf.2012.03.015>
21. T. Aubert, M.B. Assouar, O. Legrani, O. Elmazria, C. Tiusan, S. Robert, Highly textured growth of AlN films on sapphire by magnetron sputtering for high temperature surface acoustic wave applications. *J. Vac. Sci. Technol. A* **29**(2), 021010 (2011). <https://doi.org/10.1116/1.3551604>
22. Y.C. Yang, C. Song, X.H. Wang, F. Zeng, F. Pan, Giant piezoelectric d33 coefficient in ferroelectric vanadium doped ZnO films. *Appl. Phys. Lett.* **92**(1), 012907 (2008). <https://doi.org/10.1063/1.2830663>

Publisher's Note Springer Nature remains neutral with regard to jurisdictional claims in published maps and institutional affiliations.